Published in final edited form as:
*Soft Matter*. 2010 June 15; 6(20): 5045–5055. doi:10.1039/C0SM00101E.

# Hierarchically structured, hyaluronic acid-based hydrogel matrices via the covalent integration of microgels into macroscopic networks[$]

**Amit K. Jha**[1], **Manisha S. Malik**[2], **Mary C. Farach-Carson**[2,3], **Randall L. Duncan**[2,4], and **Xinqiao Jia**[1,*]

[1] Department of Materials Science and Engineerinsg, Delaware Biotechnology Institute, University of Delaware, Newark, DE 19716

[2] Department of Biological Sciences, University of Delaware, Newark, DE 19716

[3] Department of Biochemistry and Cell Biology, Rice University, Houston, TX 77251

[4] Department of Mechanical Engineering, University of Delaware, Newark, DE 19716

## Abstract

We aimed to develop biomimetic hydrogel matrices that not only exhibit structural hierarchy and mechanical integrity, but also present biological cues in a controlled fashion. To this end, photocrosslinkable, hyaluronic acid (HA)-based hydrogel particles (HGPs) were synthesized via an inverse emulsion crosslinking process followed by chemical modification with glycidyl methacrylate (GMA). HA modified with GMA (HA-GMA) was employed as the soluble macromer. Macroscopic hydrogels containing covalently integrated hydrogel particles (HA-*c*-HGP) were prepared by radical polymerization of HA-GMA in the presence of crosslinkable HGPs. The covalent linkages between the hydrogel particles and the secondary HA matrix resulted in the formation of a diffuse, fibrilar interface around the particles. Compared to the traditional bulk gels synthesized by photocrosslinking of HA-GMA, these hydrogels exhibited a reduced sol fraction and a lower equilibrium swelling ratio. When tested under uniaxial compression, the HA-*c*-HGP gels were more pliable than the HA-*p*-HGP gels and fractured at higher strain than the HA-GMA gels. Primary bovine chondrocytes were photoencapsulated in the HA matrices with minimal cell damage. The 3D microenvironment created by HA-GMA and HA HGPs not only maintained the chondrocyte phenotype but also fostered the production of cartilage specific extracellular matrix. To further improve the biological activities of the HA-*c*-HGP gels, bone morphogenetic protein 2 (BMP-2) was loaded into the immobilized HGPs. BMP-2 was released from the HA-*c*-HGP gels in a controlled manner with reduced initial burst over prolonged periods of time. The HA-*c*-HGP gels are promising candidates for use as bioactive matrices for cartilage tissue engineering.

### Keywords

Hyaluronic acid; hydrogels; particles; networks; photocrosslinking; covalent integration; BMP-2; chondrocytes

[$]This manuscript is submitted to Journal of Materials Chemistry and Soft Matter joint themed issue on Tissue Engineering.

[*]To whom correspondence should be addressed: Xinqiao Jia, 201 DuPont Hall, Department of Materials Science and Engineering, University of Delaware, Newark, DE, 19716, USA. Phone: 302-831-6553; Fax: 302-831-4545; xjia@udel.edu.

## Introduction

Hydrogels are defined as interconnected networks of macroscopic dimensions, established via a crosslinking process that renders the constituent building blocks insoluble in aqueous media. Due to their structural and functional similarities to the natural extracellular matrices (ECM), hydrogels are widely exploited as tissue engineering scaffolds.[1] Traditional bulk hydrogels are macroscopic entities consisting of nanoscale pores[2, 3] defined by the soluble polymer precursors that are randomly linked. Although these hydrogels exhibit defined shape and finite modulus, they lack the structural complexity and functional diversity seen in the natural ECM. Microgels, or nanogels, on the other hand, are hydrogel particles (HGPs) of micron- or nanometer dimensions.[4] They exhibit tunable size, large surface area, faster responses, defined nanoscopic pore size and enhanced stability. Hydrogels can be engineered to present addressable functional groups for multivalent bioconjugation and the interior network can be utilized as a drug depot.[5, 6] Unlike the bulk gels that exhibit tissue-like viscoelasticity, a microgel dispersion does not have mechanical integrity that is essential for the repair and regeneration of mechanically active tissues, such as cartilage and vocal folds.

Covalent integration of HGPs into macroscopic hydrogel networks offers an attractive strategy to overcome limitations associated with the bulk gels and HGPs. In particular, nanostructured hydrogels have been prepared using HGPs as the building blocks or crosslinkers instead of linear (or branched) soluble polymer precursors.[7, 8] Referred to as the doubly crosslinked networks (DXNs), these hydrogels exhibit two levels of crosslinking: one within the individual hydrogel particles, and the other between neighboring particles.[5] By varying the chemical and structural characteristics of the constituent building blocks, the mechanical properties and the degradation kinetics of the composite matrices can be readily modulated. Finally, therapeutically active molecules can be presented in a spatial and temporal fashion by their selective immobilization at a pre-determined locale within the composite matrix.

The goal of the current investigation is to engineer HA-based hydrogel matrices that are suitable for cartilage repair and regeneration. HA is naturally abundant in native ECM, therefore inherently biocompatible. It exhibits diverse biological functions including wound healing, morphogenesis and embryonic development.[9–11] In cartilage, HA interacts with aggrecan to form large aggregates that not only help organize the cartilage ECM but also provide compression resistance to the tissue.[12] Finally, the abundance of functional groups (OH and COOH) in HA allows for its chemical modification and covalent crosslinking to be achieved under mild conditions.[13–15] In our previous investigation, we demonstrated the utility of perlecan domain I (PlnDI)-conjugated HA HGPs for the sustained release of bone morphogenic protein 2 (BMP-2). The PlnDI-conjugated, BMP-2 loaded HGPs effectively induced the chondrogenic differentiation of mesenchymal stem cells in a high density, micromass culture.[16] In order to realize the potentials of HA hydrogels in cartilage tissue engineering, a three dimensional (3D) matrix that allows for *in situ* encapsulation and prolonged culture of primary chondrocyte *in vitro* is desirable. In the current investigation, we report the synthesis of photocrosslinkable HA HGPs and the subsequent formation of DXNs by radical polymerization. The resulting composite hydrogels were characterized in terms of their microstructures, sol fraction, water uptake, enzymatic degradation and mechanical properties. Primary bovine chondrocytes photoencapsulated in DXNs maintained rounded cell morphology and actively produced cartilage specific ECM components. BMP-2 releasing DXNs were prepared by photocrosslinking of BMP-2-loaded HGPs along with a soluble HA macromer.

## Materials and Methods

### Materials

Hyaluronic acid (HA, sodium salt, ~500 kDa) was generously donated by Genzyme Corporation (Cambridge, MA). Dioctyl sulfosuccinate sodium salt (Aerosol OT, AOT, 98%), 1-heptanol (1-HP), 2,2,4-trimethylpentane (isooctane), bovine testicular hyaluronidase (HAase, 30,000 U/mg), divinyl sulfone (DVS), (*N*,*N*-dimethylamino) pyridine (DMAP), tetrabutylammonium bromide (TBAB), 2,2-dimethoxy-2-phenylacetophenone (DMPA), 1-vinyl-2-pyrrolidinone (NVP), Alcian blue 8GX and glycidyl methacrylate (GMA) were purchased from Aldrich (Milwaukee, WI). Acetone, concentrated sulfuric acid, sodium hydroxide, carbazole and ethanol were obtained from Thermo Fisher Scientific (Waltham. MA). Recombinant human BMP-2 (rhBMP-2) and BMP-2 Quantikine ELISA kit were obtained from R&D Systems (Minneapolis, MN). Paraformaldehyde (16% in $H_2O$) was obtained from electron microscopy sciences (Hatfield, PA). Dulbecco's minimum essential medium (DMEM), fetal bovine serum (FBS), penicillin, streptomycin, and glutamine were purchased from Invitrogen (Carlsbad, CA, USA). Propidium iodide and SYTO 13 were purchased from Genway Biotech, Inc (San Diego, CA). All reagents were used as received.

### Chemical Modification of HA (HA-GMA)

HA was chemically modified with GMA following previously reported procedures.[17] To an aqueous solution of HA (15 mg/mL, 50 mL) was added DMAP (6.4 molar excess relative to HA repeats), GMA (20 molar excess) and TBAB (2.7 molar excess). The reaction was allowed to proceed under nitrogen at room temperature in the dark for 48 h. Upon addition of NaCl, the reaction mixture was added drop-wise to a large access of acetone. The white, fluffy precipitate was collected by filtration. The precipitation process was repeated twice and the final precipitate was re-dissolved in 300 mL $H_2O$ and dialyzed (MWCO 10,000) against 0.1 N NaCl for 24 h and DI $H_2O$ for another 24 h. The purified product was freeze dried and stored at 4 °C in the dark prior to use.

### Synthesis of Photocrosslinkable HA HGPs (HGP-GMA)

To synthesize HA HGPs, HA was allowed to react with DVS in inverse emulsion droplets of aqueous NaOH dispersed in isooctane and stabilized by AOT and 1-HP, as previously reported.[5, 18] After 1 h reaction, a large amount of acetone was added to the reaction mixture and HGPs were obtained by extensive washing and repeated centrifugation at 12,000 rpm, followed by drying under vacuum at room temperature. To render the resulting HGPs photocrosslinkable, the particles were dispersed in DI $H_2O$ at a concentration of 10 mg/mL. To this suspension was added GMA (40 molar excess relative to the HA repeats), along with DMAP (40 mol %) and TBAB (80 mol %). The reaction was allowed to proceed at room temperature in a nitrogen atmosphere for 96 h in the dark. The methacrylated HGPs (HGP-GMA) were washed with NaCl (5 wt%) solution, water, ethanol and acetone three times. The vacuum dried particles were stored at 4 °C in the dark prior to use.

### Hydrogel Synthesis

HA-*c*-HGP gels were prepared using HA-GMA and HGP-GMA as the macromer and crosslinker, respectively. Four mg of dry HGP-GMA were dispersed in DI $H_2O$ and the swollen particles were collected after the centrifugation at 12,000 rpm for 10 min. The particle pellet was re-dispersed in HA-GMA (0.5 mL, 2 wt%) containing 1.5 μL of the initiator solution (30% DMPA in NVP). The solution was exposed to a long wavelength UV lamp (Model 100AP, Blak-Ray) for 10 min for complete gelation. The HA-*p*-HGP gels were prepared similarly using HGP instead of HGP-GMA. Traditional bulk gels (HA-GMA) were synthesized in the absence

of hydrogel particles. Briefly, HAGMA (1 mL, 2 wt% in DI $H_2O$) was mixed with the initiator solution (3.0 μL) and the solution was subjected to UV irradiation for 10 min.

### Compositional Analysis

$^1H$ NMR spectra were recorded in $D_2O$ on a Bruker AV400 NMR spectrometer under standard quantitative conditions and were analyzed with Bruker Topspin software. All chemical shift values were calibrated using the solvent peak (from proton impurities, 4.8 ppm for $D_2O$).

### Particle Characterization

The average size and size distribution of hydrogel particles (dispersed in DI $H_2O$) were analyzed by dynamic light scattering (DLS) using Zetasizer Nano ZS (Malvern Instruments, UK). Three separate injections were analyzed and the graph reported was a representative trace. Scanning electron microscopy (SEM) images of HGP-GMA were obtained using a JSM 7400F SEM (operating voltage: 3 kV, current: 10 $\mu$A). Particles suspended in acetone were deposited on aluminum stubs, and the acetone was evaporated at room temperature.

### Hydrogel Morphology

Cryogenic SEM (CryoSEM) was applied to visualize the native hydrogel microstructure.[5, 19] Samples were frozen rapidly (≥10 000 deg/s) under high pressure (≥2000 bar) and then freeze fractured in liquid nitrogen. After water was sublimed, the specimens were coated with gold-palladium (10 mA current) at −130 °C, and subsequently viewed in a Hitachi S-4700 FESEM (Tokyo, Japan) at 1 kV (emission current: 30 $\mu$A) with a working distance of approximately 3–6 mm.

### Swelling Ratio and Sol Fraction

To measure the hydrogel sol fraction, the as-synthesized gels were allowed to swell in PBS (pH of 7.4). After 24 h of incubation at 37°C, PBS was aspirated, and the gel disks were soaked in DI $H_2O$ for another 24 h at 37°C. Hydrogels were thoroughly washed with DI water to remove the excess salt. Samples were subsequently dried by passing through graded ethanol solutions. The sol fraction was calculated from the ratio of the final dry weight and the initial solid mass used in the gel preparation. To measure the equilibrium swelling ratio, the **a**s-synthesized gels were dried by passing through degraded ethanol solutions, and the solvent was evaporated under vacuum. After the dry weight was recorded, the gel discs were immersed in PBS at 37 °C overnight and the wet weight was measured. The swelling ratio was defined as the ratio of the final wet weight to the initial dry weight. The results reported were an average from five repeated measurements.

### Mechanical Characterization

Mechanical analysis was conducted on a dynamic mechanical analyzer (RSA III instrument, TA Instruments, New Castle, DE) using a parallel plate geometry that measures the deformation as a function of normal stress. The gel disks (height: 4.0 mm and diameter: 6.3 mm) were prepared in the cell culture insert and compression tests were performed immediately upon gelation. All samples were compressed at a rate of 20%/min until fracture. Compression tests were performed in triplicate for all samples. The modulus was calculated using the initial linear portion of the stress-strain curve.

### Enzymatic Degradation

The stability of the hydrogels and hydrogel particles was evaluated in the presence of HAase. Individual hydrogel disks (~1.3 mg dry weight) were separately immersed in a HAase solution (1 mL, 5 U/ml) in PBS at pH 7.4 at 37 °C. HGPs (3 mg) were incubated at 37 °C in a HAase

solution (1 mL, 100 U/mL) in sodium acetate buffer at pH of 4.0. The supernatant was aspirated off every other day and was stored at −20 °C until further analysis. The degradation medium was replenished with freshly prepared enzyme solution. The amount of HA degraded was quantified by carbazole assay following reported procedures.[20] All analyses were carried out in triplicate and the cumulative degradation (as a % of total) was calculated by dividing the amount of uronic acid released up to a chosen measurement time with the initial dry weight the gels.

### Isolation of Primary Chondrocyte

Bovine articular cartilage was dissected from carpal joints of legs of ~1-year-old bovines and was shipped from Indiana overnight on dry ice. Immediately upon arrival, the explants were minced and subsequently digested in a Pronase solution (1 mg/mL in DMEM with 10% FBS) for 30 min at 37 °C. The explants were subsequently washed with PBS twice and incubated in a Collagenase P solution (1 mg/mL, in DMEM with 10% FBS) at 37 °C overnight under gentle agitation at 50 rpm. The digested solution was passed through a 40 or 70 μm filter, and centrifuged for 8–10 min at approximately 200 g. The supernatant then was aspirated off, and the pellet was washed twice with PBS. The cell pellet was subsequently suspended in DMEM/F-12 medium containing 1% PS, 10% FBS, 50 μg/mL sodium pyruvate and 50 μg/mL ascorbic acid. The chondrocyte viability was determined using trypan blue exclusion and dead cells (blue) were counted manually using a hemacytometer. Primary chondrocytes were plated at a confluency of 50–60% and incubated at 37 °C in a humidified atmosphere with 5% $CO_2$ with the complete media for 24 h and serum starved for another 24 h before the experiment.

### Cell Encapsulation and Cell Viability

For cell culture studies, the dialyzed HA-GMA solution was sterile filtered (0.22 μm) before being lyophilized. Hydrogel particles were exposed to a germicidal lamp in a laminar flow hood for 30 min, followed by soaking in ethanol/$H_2O$ (70%) overnight. Chondrocytes were dispersed in the precursor solutions that contained HA-GMA, HGPs and photoinitiator at a final concentration of $4\times10^6$ cells/mL. The suspension was transferred to a cell culture insert that was placed in a 24 well plate, and was exposed to the UV irradiation for 10 min. The cell-laden hydrogels were incubated at 37 °C in a humidified atmosphere with 5% $CO_2$ with 400 μL complete media. Medium was refreshed every 3 days. After 7 days of culture, the cell/gel constructs were stained with propidium iodide (1:2000 in DPBS) and SYTO 13 (1:1000 in DPBS). Images were acquired using a Zeiss Axiovert confocal microscope (Axiovert LSM 510).

### Alcian Blue Staining

The production of sulfated glycosaminoglycan (sGAG) was confirmed calorimetrically using an Alcian blue staining. After 9 days of culture, the cell/gel constructs were washed with PBS and fixed in 4% (v/v) paraformaldehyde for 4 h. The samples subsequently were stained with Alcian blue (0.5 wt% in 3% (v/v) glacial acid) at pH 1.0. After overnight incubation at ambient temperature, the constructs were thoroughly rinsed with distilled water and were photographed with a digital camera attached to a Nikon microscope (Coolpix 990, Nikon, Kanagawa, Japan). Cell-free hydrogels were subjected to the same staining protocol as the controls.

### BMP-2 Loading and *in vitro* Release

The BMP-2 loading buffer was prepared from PBS, with the addition of 0.1% BSA, 1% Penicillin-Streptomycin (PS) and 0.1mM phenylmethylsulfonyl fluoride (PMSF). One mg of hydrogel particles were dispersed in 200 μL of loading buffer containing 200 ng rhBMP-2. The suspension was left overnight at 4 °C. The BMP-2 loaded hydrogel particles were collected by centrifugation at 12,000 rpm for 10 min and the supernatant was removed for BMP-2

quantification using BMP-2 ELISA kit following the manufacture's instruction. The amount of BMP-2 loaded into the hydrogel particles was determined by subtracting the amount of BMP-2 remaining in the supernatant from that initially added. BMP-2 loaded particles thus prepared were immediately used for hydrogel formation following procedures described above. For BMP-2 release study, hydrogel disks or particles were incubated in the release media (CMRL 1066, with 1% PS, 400 μL) at 37 °C. At predetermined time points, the supernatant was collected and an equal amount of release media was added. The amount of BMP-2 in the release medium was measured using the BMP-2 ELISA kit. All measurements were carried out in triplicate.

### Statistical analysis

All quantitative measurements were performed on 3 replicates. All values are expressed as means ± standard deviations (SD). Statistical significance was determined using a two-tailed student t-test. A p value of less than 0.05 was considered to be statistically different.

## Results and Discussion

The goal of the current investigation was to engineer HA-based hydrogels that are hierarchically structured, mechanically robust and biologically active, suitable for use as 3D matrices for *in vitro* culture of differentiated primary chondrocytes. Our hydrogel systems synergistically combine the unique attributes of microgels and traditional bulk gels by photocrosslinking HA hydrogel particles with a soluble, HA macromomer (HA-GMA) (Figure 1). Photocrosslinking is advantageous over other chemical approaches because it permits rapid gelation under physiological temperature and pH with accurate spatial controls. Direct photoencapsulation of cells in a synthetic hydrogel creates a construct with defined nanoscale topography and tunable viscoelasticity that promote control of cell-matrix interaction, cell differentiation, cell migration and neotissue formation. Photocrosslinking has proven to be an efficient method for encapsulation and growth of various types of cells including chondrocytes[21–24] and embryonic stem cells.[25, 26]

### Synthesis and Characterization of Photocrosslinkable HA HGPs

Soluble HA macromer (HA-GMA) was synthesized successfully following established procedure.[17] An 11% methacrylation was determined by comparing the relative integrations of the vinyl protons (~5.6 and ~6.1 ppm) and HA's methyl proton (NAc-$CH_3$, ~1.8 ppm) (Figure S1A). Separately, HA HGPs were synthesized by covalent crosslinking of HA with DVS within the inverse emulsion droplets of water/isooctane that were stabilized by AOT and 1-heptanol. The crosslinking occurs between the primary OH groups of HA and the vinyl groups in DVS under basic conditions.[27] The resulting HA HGPs were spherical in shape and exhibited smooth surfaces and an average diameter of ~1 μm.[5, 18] HA HGPs were subsequently methacrylated (HGP-GMA) by reacting with a large excess of GMA in DI $H_2O$ in the presence of tertiary amine and a phase transfer agent. Both trans-esterification reaction between the residual, primary hydroxyls in HGPs and the ester group of GMA, and the carboxylate-initiated ring-opening conjugation with GMA exist under the reaction conditions employed.[28] The presence of hydrated, nano-scale pores in HA HGPs, combined with the small molecular dimension of GMA and the presence of phase transfer agent, suggest that the chemical modification occurred throughout the bulk of the particles, rather than being limited to the particle surfaces.

To confirm the presence of the methacrylate groups in HGP-GMA, particles were solublized in acidic medium prior to $^1$H NMR analysis. HGPs and GMA treated under the same conditions were included as the controls. The $^1$H NMR spectrum for the hydrolyzed HGPs (Figure S1B) presents the characteristic signals of the degraded HA products, possibly consisting of

oligosaccharides of various molecular weights. No addition reaction occurred between HCl and the unsaturated double bond in GMA under the degradation conditions since the vinyl protons are clearly present (~5.7 and ~6.2 ppm) and the integration ratio between the vinyl protons and the methyl protons ($CH_3$, 2 ppm) is close to 2/3 (Figure S1C). Simple mixing of GMA with HA HGPs in the absence of the catalyst and the phase transfer agent did not lead to the conjugation of the methacryalte group as evidenced by the absence of the vinyl protons in the degraded particles (data not shown). In the presence of DMPA and TBAB, HGPs were successfully methacrylated after 96 h of reaction. The characteristic vinyl protons, although shifted to a higher field, are clearly visible after HGP-GMA was degraded (Figure S1D). The shift of the vinyl protons as compared to GMA is a consequence of the alteration of the chemical environment upon degradation and chemical conjugation. [29] A simple gelation experiment was conducted to further confirm the crosslinkability of HA HGP-GMA (Supporting Information). Specifically, when acrylamide was radically polymerized in the absence of HGP-GMA, a polyacrylamide solution was obtained (Figure S2). When HGP-GMA was introduced in the monomer solution, a visoealstic gel was formed (Figure S2). Collectively, our results confirmed that HGPs were properly methacrylated.

Figure 2 shows a typical scanning electron micrograph of HGP-GMA, confirming the presence of well-defined spherical particles with relatively narrow size distribution. Quantitative particle size analysis by DLS (Figure 3) revealed an average diameter of 1.00 ± 0.08 μm for HGP-GMA. The DLS traces for HGP and HGP-GMA essentially overlapped, indicating that the chemical modification did not alter the size and structure of the hydrogel particles. Particle degradation is not likely to occur during the modification process. The crosslinkable HGPs can be consistently synthesized and the dry particles can be readily dispersed in water.

## Hydrogel Micrstructure

With HA-GMA and HGP-GMA in hand, we investigated the formation of 3D macroscopic hydrogels via a radical polymerization. In the presence of UV irradiation, DMPA fragmented into radicals that propagate along HA-GMA and HGP-GMA via a chain mechanism. The resulting hydrogels contain HA chains, HGPs and kinetic chains of poly(methacrylic acid). Stable hydrogel disks with defined shapes were obtained after 10 min of UV irradiation. While the HA-GMA gels are optically clear, the inclusion of micron sized hydrogel particles in the HA-GMA gave rise to semi-opaque gels (Figure 4), with HGPs homogeneously distributed throughout the secondary gel matrix. Prolonged incubation of both types of gels in DI $H_2O$ did not alter their physical appearance, indicating the absence of particle diffusion.

Although HA-*p*-HGP and HA-*c*-HGP-gels appear similar to the naked eye, their structures differ at microscopic levels. CryoSEM was employed in place of traditional SEM so as to preserve the innate hydrogel microstructures without creating artifacts during sample preparation. Typical CryoSEM images for HA-GMA, HA-*p*-HGP and HA-*c*-HGP gels are shown in Figure 5. It is clear that the HA-GMA gels are composed of homogeneously distributed pores of submicron size range. Both HA-*p*-HGP and HA-*c*-HGP gels contain densely crosslinked, nanoporous HGPs surrounded by a loosely interconnected, secondary matrix that exhibited similar morphology as the HA-GMA matrix. When HGPs were physically entrapped in HA-GMA matrix, a depletion zone around the hydrogel particles (Figure 5B) was created even though the HGPs and the secondary network were of the same chemical make-up. In the case of HA-*c*-HGP gels, the secondary network is connected to the particle covalently as evidenced by the fibrilar structure bridging the particle surface and the secondary matrix. A diffuse interphase between individual particles and the secondary matrix was created (Figure 5C). The highly reactive radicals, once generated photochemically, immediately react with the nearest and the most accessible π-bond to form the propagating radicals.[30] It is highly unlikely for the HA chains carrying the reactive radicals to diffuse deep into the HGPs during the

gelation process because of the large molecular dimensions of branched or partially crosslinked HA-GMA, the small mesh size of HGPs,[5, 16] the short half life of radicals and the rapid reaction kinetics. Collectively, our results confirm that the radical species along the HA-GMA chains are capable of propagating through the methacrylate groups anchored on the particle surface, establishing covalent linkages between the particles and the surrounding, secondary matrix.

## Hydrogel Swelling and Sol Fraction

The equilibrium water uptake by the hydrogels was measured after overnight immersion in PBS at 37 °C. Hydrogel sol fraction was evaluated by comparing the dry mass of the hydrogels before and after 24-h equilibration in PBS, during which the physically entangled HA chains that are not immobilized to the network (sol fraction) diffused out of the gels. It can be seen from Figure 6 that the HA-GMA gels exhibit an average swelling ratio of 62 ± 3.6 and a sol fraction of 34 ± 13 %. Physical inclusion of HGPs in the HA-GMA matrix led to a reduction in both swelling ratio (43 ± 4) and the sol fraction (25 ± 10%). Hydrogels containing covalently integrated HGP-GMA exhibit the lowest water uptake (38 ± 2). Close to 90 ± 5.8% of macromers were effectively incorporated in the final HA-*c*-HGP gel networks.

It is not surprising that HA-*c*-HGP gels exhibited a lower sol fraction values and swelled to a lesser degree as compared to HA-GMA gels because they were formulated at a higher HA concentration (28 mg/mL vs. 20 mg/mL total HA for HA-c-HGP and HA-GMA gels, respectively). Interestingly, the HA-*c*-HGP gels exhibited significantly ($p<0.05$) lower sol content than the HA-*p*-HGP gels although they contained the same amount of HA-GMA and HGPs. As discussed above, the large size of the particles prohibits them from diffusing out of the matrix readily. The low sol fraction observed for HA-*c*-HGP gels suggests that a relatively higher amount of HA chains were immobilized to the covalent network, a direct consequence of a more efficient crosslinking process. The multiple methacrylate groups on the surface of the spherical particles were well exposed and readily accessible for chain polymerization. In an aqueous medium at 20 mg/mL, the methacrylate groups in HA-GMA may be buried because of the hydrophobic nature of the GMA groups and the flexibility of the HA chain. In other words, the spherical, microscopic objects are more efficient crosslinkers than their soluble counterparts. The crosslinkable HGPs essentially rescued the propagating HA-GMA chains, leading to lower sol content in the final gels. Such rescuing mechanism is absent in HA-*p*-HGP gels due to the lack of addressable functional groups on the unmodified HA HGPs. The covalent integration of crosslinkable HGPs in a secondary network offers an effective means to reduce the amount of soluble polymer chains that are physically entangled in the network but diffuse out later on.[5]

## Hydrogel Degradation and Mechanics

In natural ECM, hyaluronidase (HAase) is responsible for HA turnover, which can affect cell migration, differentiation, and matrix catabolism. HAase catalyzes the random scission of 1,4-linkages between 2-acetamido-2-deoxy-b-D-glucose and D-glucose residues in native HA.[9] The optimal pH for HAase is 4.5–6. The enzymatic stability of HGPs and various hydrogels were monitored by carbazole assay[20] and the cumulative degradation profiles were plotted as the overall percentage of uronic acid detected as a function of degradation time (Figure 7). At low HAase concentration under physiological pH, minimal degradation was detected for HGPs. To accelerate the degradation, HGPs were suspended in 100 U/mL in a sodium acetate buffer at pH 4.0. The percent degradation as a function of incubation time (Figure 7) showed an initial linear loss of HA at a rate of ~9% per day up to 6 days. Thereafter, the degradation rate leveled off. Approximately 25 wt% of HGPs was left after 15 days of degradation.

When exposed to 5 U/mL HAase at pH 7.4, the bulk gels progressively became smaller and more fragile. The gel disks lost their coherence and were fragmented after 6 days of incubation.

Approximately 73.0 ± 12.5% degradation was detected at day 4 and complete degradation was observed at day 10 (Figure 7). Incorporation of HGPs in the HA-GMA matrix, both physically and covalently, resulted in composite matrices with improved enzymatic stability. Both types of gels degraded at a slower rate than the HA-GMA gels, and the uronic acid produced at day 4 accounted for approximately 55.4 ±4.6% and 46.0 ± 2.5% of the initial weight HA, respectively (Figure 7). Unlike the bulk gels, particle-containing hydrogels maintained their macroscopic geometry and structural integrity throughout the course of the degradation study. The opaque gel disks remained present on day 15, although their size and thickness were decreased.

The ability of HAase to degrade the HA-based hydrogels suggests that the chemical modification and covalent crosslinking did not significantly alter the biological identity of HA. A swelling ratio of 62 for the HA-GMA gels, as compared to 5 for the HGPs, clearly indicates a less crosslinked network for the former. The presence of residual surfactant molecules on the particle surface may limit the ability of HAase to access the particles for surface erosion. It is speculated that the hydrogels degrade predominately via surface erosion mechanism due to the diffusion restriction of HAase into the interior of the gel.[31] The addition of densely crosslinked HGPs in the bulk HA-GMA matrix naturally results in an enhanced enzymatic stability. The covalent coupling between HGP-GMA and the HA-GMA further enhances the enzymatic stability of the resulting matrices. Degradation characteristic of hydrogel matrices plays an essential role in modulating cellular functions. Our motivation in combining the two cross-linking mechanisms stems from our interest in only very lightly covalently crosslinking these hydrogels to stabilize the particles without unnecessarily increasing the modulus of the hydrogel, and to provide opportunities for erosion of the hydrogels upon regeneration of native tissues *in vivo*.

We are interested in evaluating the applicability of the HA-based hydrogels with covalently integrated HGPs for cartilage repair. The unique viscoealstic properties of hydrated cartilage allow it to withstand compressive forces regularly at frequencies of 0.1–3 Hz.[32,33] Representative stress versus strain curves for the three types of gels investigated are plotted in Figure 8. Linear viscoelastic regions were observed at strains <20%. The up-turn, commonly observed in hydrogel materials at [34, 35] high strain (>30%), can be attributed to the material densification and/or strain hardening.[36, 37] The compressive modulus, calculated by taking the slope of the stress-strain curve in the linear region, for HA-GMA, HA-*p*-HGP and HA-*c*-HGP gels was 15.7± 1.8 kPa, 22.7 ± 1.2 kPa and 18.5 ± 1.2 kPa, respectively (Figure 8). The addition of densely crosslinked hydrogels particles to HA-GMA matrix led to a moderate increase in the compressive modulus and fracture strain. Unlike the traditional composites where the fillers are stiff, inorganic nanoparticles, the inclusion of small amount (21% of the total mass) of hydrogel particles into a soft hydrogel matrix does not lead to a dramatic change in matrix stiffness. Hydrogels containing physically trapped HGPs are statistically stiffer ($p \leq 0.05$) than those containing covalently integrated particles. When the HA-*p*-HGP gels were compressed, the mechanical force applied to the gels could not be directly transmitted to the entrapped particles due to the absence of particle-matrix coupling and the presence of the depletion zone around the particles. On the other hand, the presence of the covalent linkages between the individual particles and their surrounding matrix in HA-*c*-HGP gels permits the external forces to be directly transmitted to the particles, resulting in particle deformation without compromising the overall matrix strength. We have observed the force-induced particle deformation in a HA-based, doubly crosslinked networks prepared by direct mixing of aldehyde presenting HGPs and a soluble HA derivative carrying hydrazide groups.[5]

### 3D Chondrocyte Culture

Although cartilage has a relatively simple structure with limited cell diversity, absence of vascularity and innervations, successful engineering of functional cartilage *in vitro* has not been realized, due in part to the limited regenerative capacity of chondrocytes.[32] In order to rebuild the articular cartilage, complexity of interactions between cells, matrix and morphogenic factors needs to be recapitulated *in vitro*. In this study, we evaluate the potential of HA-*c*-HGP hydrogels for cartilage repair by *in situ* encapsulation and 3D culture of primary bovine chondrocytes. Live/dead assay after 7 days of culture detected minimal numbers of dead cells, indicating the biocompatible nature of the encapsulation process as well as the resulting matrices (Figure 9). Furthermore, cells retained chondrocytic spherical morphology in 3D, whereas those cultured on 2D TCPS adopted a spread-out, spindle shaped morphology, suggesting differentiation (Figure 9). Chondrocytes were dispersed uniformly throughout the gels without severe aggregation as encountered in other macroporous HA gels. [38] The production of sulfated glycosaminoglycan (sGAG) was analyzed by Alcian blue staining. Alcian blue is known to selectively stain sGAG rather than HA at low pH. As expected, the control HA gels without the cells showed a minimal background staining. The Alcian blue staining for HA-*p*-HGP and HA-*c*-HGP gels revealed the presence of HGPs homogeneously distributed in the secondary matrix, in agreement with visual inspection (see above). The cell/gel constructs exhibit intense and robust blue staining, indicative of sGAG accumulation and neocartilage formation. Chondrocytes encapsulated in HA-GMA gels are clearly visible (Figure 10A). Because the embedded cells appear similar microscopically to the hydrogel particles, both in size and shape, they cannot be easily identified in the composite matrices by Alcican blue staining. All three types of hydrogel investigated exhibit similar levels of blue staining, irrespective of their composition and microstructure.

Our results show that freshly isolated bovine articular chondrocytes underwent de-differentiation to a fibroblast-like phenotype when cultured in monolayer. When encapsulated in the 3D microenvironment created by HA and HGPs, chondrocytes are able to re-differentiate and express their original phenotype. In the absence of soluble factors or biophysical stimulations, primary chondrocytes residing in the HA matrix produced remarkable amounts of sGAG within a short culture time. Therefore, the HA matrices described here not only provide mechanical support for the cells but also actively modulate their *in vitro* behaviors through cell-matrix interaction. It is well documented that binding of chondrocyte to HA by the CD44 receptor affects chondrocyte functioning and is essential for cartilage homeostasis. Blocking of CD44 HA binding on chondrocytes results in degradation of the cartilage matrix. [39, 40] It is highly possible that the chemical modification did not significantly alter the ability of HA to bind CD44 and to elicit chondrogenic activities.[41, 42] The lack of difference in live/dead assay and Alcian blue staining for chondrocytes cultured in HA-GMA, HA-*p*-HGP and HA-*c*-HGP gels in short term, static culture conditions does not imply that cells residing in these matrices do not “feel” and respond to the structure differences. These results, although preliminary, underscore the potential of HA-*c*-HGP gels as scaffolds for cartilage tissue engineering.

### Growth Factor Release

The HA-based hydrogel particles are intended not just as passive, cell delivery scaffolds; rather as bioactive matrices that provide local and sustained delivery, with release kinetics dependent on the crosslinking strategies and encapsulation methods used. The biologically active compound that is of interest to us is BMP-2. BMP-2 is the cytokine that most effectively enhances the recruitment of mesenchymal stem cells (MSCs) to cartilage condensations, modulates expansion of condensation size, and initiates BMP-dependent signaling cascades in mesenchymal progenitor cells for the induction of chondrogenesis.[43] The importance of BMP-2 activity for normal joint formation, articular cartilage development and maintenance,

the chondrogenic activity of BMP-2 when applied to MSC cultures, and the encouraging *in vivo* outcomes have been well-documented.[33, 44, 45]

BMP-2 releasing matrices were prepared by photocrosslinking of HA-GMA in the presence of BMP-2-loaded HGPs (77.5 ± 4.0 ng per mg HGPs). The presence of loaded BMP-2 did not interfere with the gelation process. Stable gel discs with the same compression properties were obtained after 10 min UV irradiation (data not shown). Protein exclusion experiments using stable, globular proteins with molecular dimensions ranging from 3.0 to 10.2 nm revealed that HA HGPs had an average pore size of 5.5–7.0 nm.[5] With an apparent molecular weight of 26 kDa and a pI value of 8.21, [46] BMP-2 was readily driven into the interior of HGPs via ion exchange.

*In vitro* BMP-2 release from HA-*p*-HGP and HA-*c*-HGP gels was evaluated by incubating the hydrogel disks in a physiological buffer for up to 15 days in the absence of any enzyme. BMP-2 loaded HGPs were included as the controls. Our results (Figure 11) showed that the BMP-2 release kinetics strongly depended on the hydrogel microstructures. The release curves for HGPs and the HA-*p*-HGP gels are characterized with an initial burst from day 0 to day 3, followed by a release at a much slower rate over 10 days. Physical encapsulation of BMP-2 loaded particles in a secondary matrix introduced additional pathways for the growth factor molecules to diffuse through, hence a shift of the overall release curve to a lower cumulative release at any given time points. After 3 days, a cumulative release of 68.9 ± 5.4% and 46.1 ± 0.9% was observed for HGPs and P-gels, respectively. After 13 days of incubation, a total of 84.9 ± 9.0% and 52.3 ± 0.7% of initially bound BMP-2 was released from HGP and HA-*p*-HGP gels, respectively. The slower release observed after the initial burst is due to the association of HA with BMP-2 at pH 7.4, presumably due to the ionic bonds between the negatively charged HA and positively charged BMP as well as multiple hydrogen-bonding interactions between HA and BMP-2.[47]

Contrarily, when BMP-2 loaded HGPs were covalently integrated in a secondary, HA-based matrix, a sustained release with a significantly reduced initial burst was observed (Figure 11). After 3 days of incubation, only 10.3±6.4% BMP-2 initially loaded BMP-2 was released. After 15 days of incubation, 55.7±10.2% of BMP-2 still remained bound to the matrix. The experiments were terminated before 100% release was achieved. Overall, the HA-*c*-HGP gels maintained a steady state of BMP-2 over the entire course of the experiments with a cumulative release of 3.0%/day. In our previous studies, we demonstrated that HA HGPs[16] or polylactic acid-based scaffolds[44], when decorated with heperan sulfate bearing PlnDI, were capable of sustained release of BMP-2 in linear fashion. Both systems supported chondrogenetic differentiation of multipotential mouse embryonic mesenchymal cells, C3H10T1/2. In the current investigation, we show that the same level of control was achieved by covalent integration of BMP-2 loaded HGPs in a secondary matrix, without having to resort to heperan sulfate proteoglycan. The kinetic chains established between the HGPs and the secondary HA-GMA matrix provided a reinforcement mechanism that is conducive to reaching a stable and slow release pattern of BMP-2. It is well established that uncontrolled burst release of growth factors results in pathological conditions and inflammatory responses that hamper the effective tissue repair. The ability of the HA-*c*-HGP gels to provide near zero-order release of growth factor suggests the utility to control the functions of cells embedded locally within the 3D matrices. Such release kinetics is not unique for BMP-2; indeed, a small molecular weight model drug, rhodamine 6G, when loaded into the HGPs, can also be released from HA-*c*-HGP gels in a linear, sustained fashion [18]. We speculate that controlled release of other therapeutically active macromolecules can be achieved by covalent integration of macromolecule-loaded HGPs in a secondary matrix. In the current investigation, BMP-2 release was only quantified in terms of the relative amount. Future studies aim to determine

the appropriate dosage required for enhanced cellular outcomes and to assess the biological activities of the released BMP-2 to chondrocytes entrapped in the hydrogels.

### Conclusion

In this report, we describe a novel hydrogel system that contains hydrogel particles (HGPs) covalently integrated in a secondary hydrogel matrix (HA-*c*-HGP gels). HA HGPs were synthesized by an inverse emulsion polymerization process via an addition reaction between HA and DVS. The resulting particles were rendered photocrosslinkable by chemical modification with GMA (HGP-GMA). UV-initiated, radical polymerization of soluble HA macromer (HA-GMA) in the presence of HGP-GMA produced a hierarchically structured composite matrix. The presence of covalent coupling between HGPs and the secondary matrix was confirmed by CryoSEM. Compared to the traditional bulk gels (HA-GMA gels) with the same chemical make-up, the HA-*c*-HGP gels contained a lower sol fraction, swelled to a lesser extent and were enzymatically more stable. The compressive modulus for HA-GMA, HA-*p*-HGP and HA-c-HGP gels were determined to be 15, 22 and 19 kPa, respectively. Primary chondrocytes photo-encapsulated in the HA-*c*-HGP matrices maintained high cell viability and exhibited healthy chondrocytic shape. The 3D microenvironment created by the HA building blocks is conducive to sGAG production and neocartilage formation. When the immobilized HGPs were used as the growth factor depot, BMP-2 was released from the HA-*c*-HGP gels linearly in a sustained manner. Follow-up studies beyond the scope of this work will examine long term culture of chondrocytes under physiologically relevant environments using HA matrices that exhibit hierarchical features, defined mechanical strength and spatial/temporal presentation of morphogenic factors.

## Supplementary Material

Refer to Web version on PubMed Central for supplementary material.

## Acknowledgments

The authors wish to acknowledge Dr. Michael Mackay and Jon Seppala for their assistance with the mechanical testing, Dr. Kirk Czymmek and Deborah Powell for their instructions on CryoSEM and Dr. Stephen Trippel and Albert Gar for providing fresh bovine cartilage. We thank Genzyme for the generous gift of HA. This work was supported in part by NIH from Grants R01 DC008965 (NIDCD, to XJ and RLD) and P20-RR016458 (NCRR, to MCFC).

## References

1. Yu L, Ding JD. Chem Soc Rev 2008;37:1473. [PubMed: 18648673]
2. Kong HJ, Alsberg E, Kaigler D, Lee KY, Mooney DJ. Adv Mater 2004;16:1917.
3. Freudenberg U, Hermann A, Welzel PB, Stirl K, Schwarz SC, Grimmer M, Zieris A, Panyanuwat W, Zschoche S, Meinhold D, Storch A, Werner C. Biomaterials 2009;30:5049. [PubMed: 19560816]
4. Zhang Y, Zhu W, Wang BB, Ding JD. J Control Release 2005;105:260. [PubMed: 15913826]
5. Jha AK, Hule RA, Jiao T, Teller SS, Clifton RJ, Duncan RL, Pochan DJ, Jia XQ. Macromolecules 2009;42:537. [PubMed: 20046226]
6. Oh JK, Lee DI, Park JM. Prog Polym Sci 2009;34:1261.
7. Bencherif SA, Siegwart DJ, Srinivasan A, Horkay F, Hollinger JO, Washburn NR, Matyjaszewski K. Biomaterials 2009;30:5270. [PubMed: 19592087]
8. Gan TT, Zhang YJ, Guan Y. Biomacromolecules 2009;10:1410. [PubMed: 19366198]
9. Garg, HG.; Hales, CA. Chemistry and Biology of Hyaluronan. Oxford: Elsevier Ltd; 2004.
10. Knudson CB, Knudson W. Faseb J 1993;7:1233. [PubMed: 7691670]
11. Laurent TC, Fraser JRE. Faseb J 1992;6:2397. [PubMed: 1563592]
12. Knudson CB, Knudson W. Semin Cell Dev Biol 2001;12:69. [PubMed: 11292372]
13. Luo Y, Kirker KR, Prestwich GD. J Control Release 2000;69:169. [PubMed: 11018555]

14. Bulpitt P, Aeschlimann D. J Biomed Mater Res Part A 1999;47:152.
15. Gurski LA, Jha AK, Zhang C, Jia XQ, Farach-Carson MC. Biomaterials. 2009
16. Jha AK, Yang WD, Kirn-Safran CB, Farach-Carson MC, Jia XQ. Biomaterials 2009;30:6964. [PubMed: 19775743]
17. Jia XQ, Burdick JA, Kobler J, Clifton RJ, Rosowski JJ, Zeitels SM, Langer R. Macromolecules 2004;37:3239.
18. Sahiner N, Jha AK, Nguyen D, Jia XQ. J Biomater Sci-Polym Ed 2008;19:223. [PubMed: 18237494]
19. Farran AJE, Teller SS, Jha AK, Jiao T, Hule RA, Clifton RJ, Pochan DP, Duncan RL, Jia XQ. Tissue Eng Part A 2010;16:1247. [PubMed: 20064012]
20. Bitter T, Muir HM. Anal Biochem 1962;4:330. [PubMed: 13971270]
21. Chung C, Mesa J, Miller GJ, Randolph MA, Gill TJ, Burdick JA. Tissue Eng 2006;12:2665. [PubMed: 16995800]
22. Bryant SJ, Bender RJ, Durand KL, Anseth KS. Biotechnol Bioeng 2004;86:747. [PubMed: 15162450]
23. Bryant SJ, Davis-Arehart KA, Luo N, Shoemaker RK, Arthur JA, Anseth KS. Macromolecules 2004;37:6726.
24. Elisseeff J, McIntosh W, Anseth K, Riley S, Ragan P, Langer R. J Biomed Mater Res Part A 2000;51:164.
25. Marklein RA, Burdick JA. Adv Mater 2010;22:175. [PubMed: 20217683]
26. Burdick JA, Vunjak-Novakovic G. Tissue Eng Part A 2009;15:205. [PubMed: 18694293]
27. US Pat Appl Pat. 4, 636, 524. 1987.
28. Bencherif SA, Srinivasan A, Horkay F, Hollinger JO, Matyjaszewski K, Washburn NR. Biomaterials 2008;29:1739. [PubMed: 18234331]
29. Leach JB, Bivens KA, Patrick CW, Schmidt CE. Biotechnol Bioeng 2003;82:578. [PubMed: 12652481]
30. Odian, G. Principles of Polymerization. John Wiley & Sons, Inc; Hoboken, NJ: 2004.
31. Liu YC, Shu XZ, Prestwich GD. Biomaterials 2005;26:4737. [PubMed: 15763253]
32. Goldring MB, Goldring SR. J Cell Physiol 2007;213:626. [PubMed: 17786965]
33. Goldring MB, Tsuchimochi K, Ijiri K. J Cell Biochem 2006;97:33. [PubMed: 16215986]
34. Gong JP, Katsuyama Y, Kurokawa T, Osada Y. Adv Mater 2003;15:1155.
35. Grieshaber SE, Farran AJE, Lin-Gibson S, Kiick KL, Jia XQ. Macromolecules 2009;42:2532. [PubMed: 19763157]
36. Miquelard-Garnier G, Creton C, Hourdet D. Soft Matter 2008;4:1011.
37. Calvert P. Adv Mater 2009;21:743.
38. Kang JY, Chung CW, Sung JH, Park BS, Choi JY, Lee SJ, Choi BC, Shim CK, Chung SJ, Kim DD. Int J Pharm 2009;369:114. [PubMed: 19059468]
39. van der Kraan PM, Buma P, van Kuppevelt T, van den Berg WB. Osteoarthritis Cartilage 2002;10:631. [PubMed: 12479385]
40. Ishida O, Tanaka Y, Morimoto I, Takigawa M, Eto S. J Bone Miner Res 1997;12:1657. [PubMed: 9333126]
41. Grigolo B, De Franceschi L, Roseti L, Cattini L, Facchini A. Biomaterials 2005;26:5668. [PubMed: 15878372]
42. Chung C, Burdick JA. Tissue Eng Part A 2009;15:243. [PubMed: 19193129]
43. Hall BK, Miyake T. Bioessays 2000;22:138. [PubMed: 10655033]
44. Yang WD, Gomes RR, Brown AJ, Burdett AR, Alicknavitch M, Farach-Carson MC, Carson DD. Tissue Eng 2006;12:2009. [PubMed: 16889529]
45. Farach-Carson MC, Hecht JT, Carson DD. Crit Rev Eukaryot Gene Expr 2005;15:29. [PubMed: 15831077]
46. Winn SR, Uludag H, Hollinger JO. Adv Drug Deliv Rev 1998;31:303. [PubMed: 10837631]
47. Crouzier T, Ren K, Nicolas C, Roy C, Picart C. Small 2009;5:598. [PubMed: 19219837]

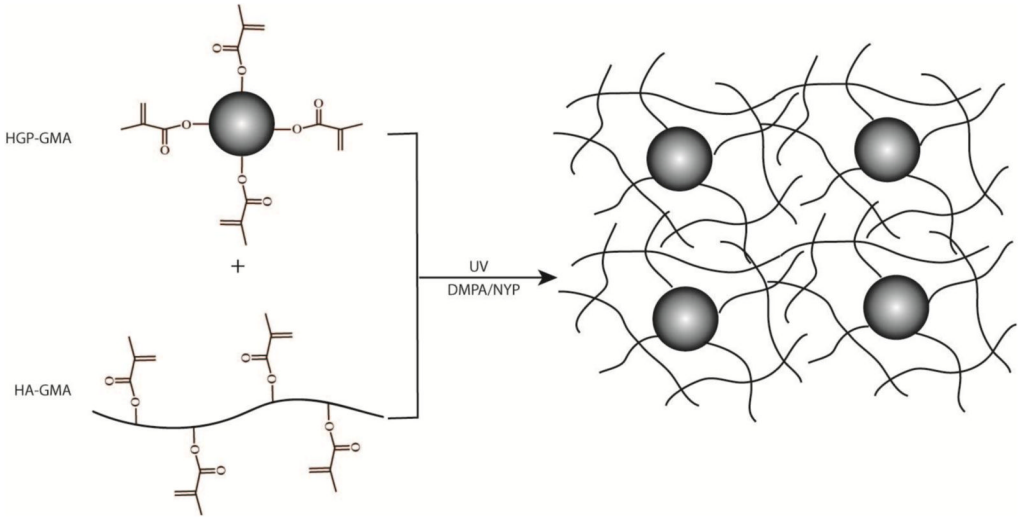


**Figure 1.**
Schematic representation of the formation of HA-*c*-HGP gels via the covalent integration of methacrylated HA hydrogel particles (HGP-GMA) into a secondary, radically crosslinked HA-GMA matrix. Not drawn to scale.

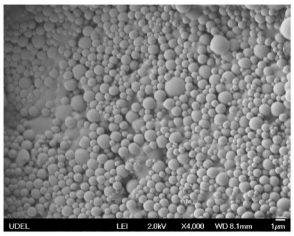


**Figure 2.**
Representative scanning electron micrograph of HGP-GMA.

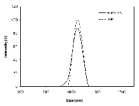

**Figure 3.**
The average size and size distribution of HGP (dotted line) and HGP-GMA (solid line) as determined by DLS. Particles were diluted in DI $H_2O$ at a concentration of ~0.1 mg/mL for the analysis. Three separate runs were carried out on each type of particle. For clarity purposes, only one representative distribution curve was shown for each type of particles.

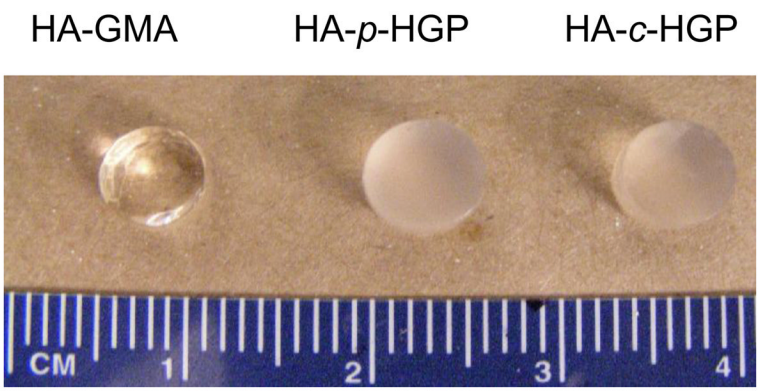


**Figure 4.**
Typical appearance of HA-GMA (left), HA-*p*-HGP (middle) and HA-*c*-HGP (right) gels.

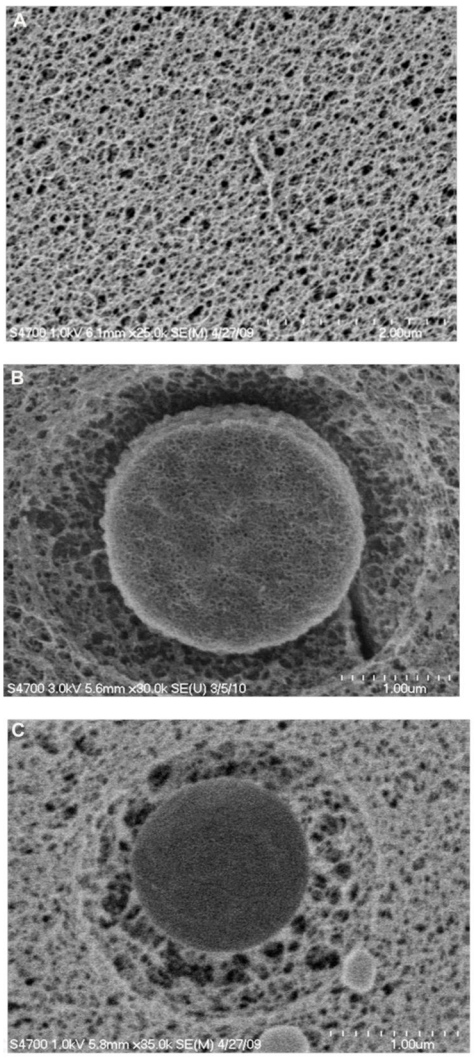


**Figure 5.**
CryoSEM images of HA-GMA (A), HA-*p*-HGP (B) and HA-*c*-HGP (C) gels.

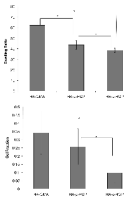

**Figure 6.**

Top: Equilibrium swelling ratio as a function of hydrogel composition. #,∉,*: The swelling ratio values for HA-GMA, HA-*p*-HGP and HA-*c*-HGP gels were significantly different from each other, $p \leq 0.05$. Bottom: Sol fraction as a function of hydrogel composition, #: The sol fraction for HA-GMA gels was significantly different from that for HA-*c*-HGP gels, $p \leq 0.05$; *: The sol fraction for HA-p-HGP gels was significantly different from that for HA-*p*-HGP gels, $p \leq 0.05$.

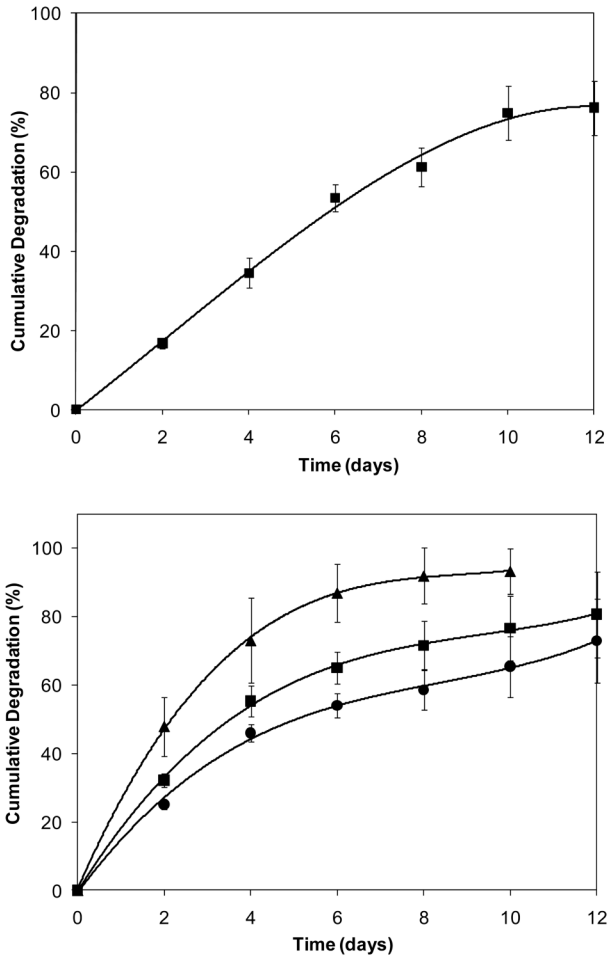


**Figure 7.**

Enzymatic degradation measured by carbazole assay. Top: Cumulative degradation of HA HGPs in 100 U/mL HAase solution at pH 4.0. Bottom: Cumulative degradation of HA-GMA gels (▲), HA-*p*-HGP gels (■) and HA-*c*-HGP gels (●) in 5 U/mL HAase solution at pH 7.4. Uronic acid release from HA-GMA gels was significantly different from its release from HA-*p*-HGP and HA-*c*-HGP gels are all times, $p \leq 0.05$.

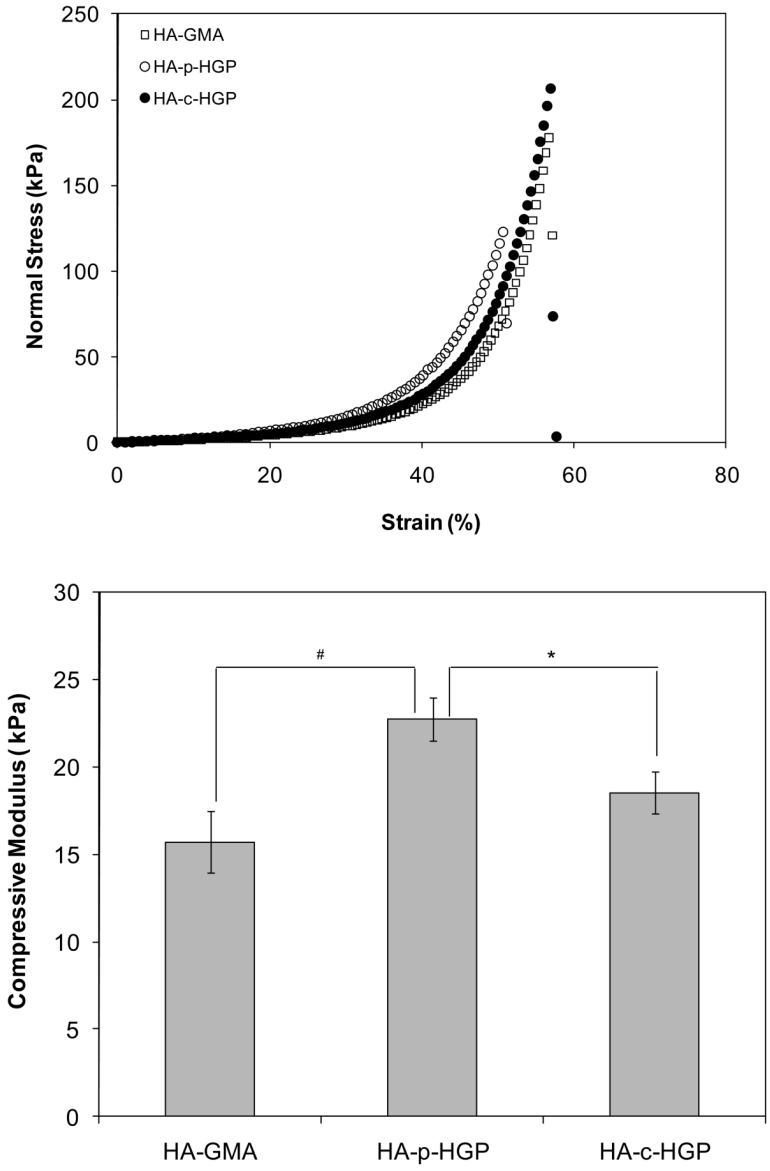


**Figure 8.**

Mechanical properties of various HA-based hydrogels. Top: Representative stress-strain curves for HA-GMA gels (□), HA-*p*-HGP gels (○) and HA-c-HGP gels (●). Bottom: Average compressive modulus for various HA networks. #: The compressive modulus for HA-*p*-HGP was significantly different from that for HA-GMA, $p \leq 0.05$; *: The compressive modulus for HA-*p*-HGP was significantly different from that for HA-*c*-HGP, $p \leq 0.05$.

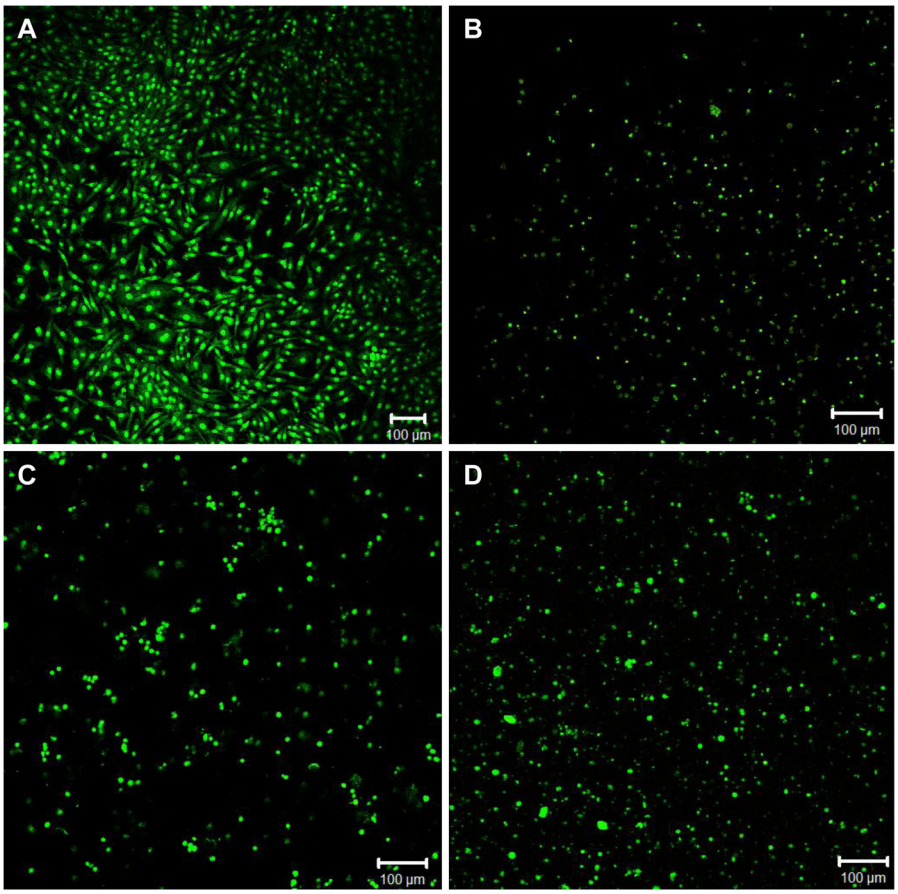


**Figure 9.**
Representative live/dead staining of primary bovine chondrocytes cultured on 2D TCPS (A) and in 3D HA matrices, including HA-GMA gels (B), HA-*p*-HGP gels (C) and HA-*c*-HGP gels (D). Live (green) and dead (red) cells were stained with SYTO 13 and propidium iodide, respectively. Scale bars 100 μm

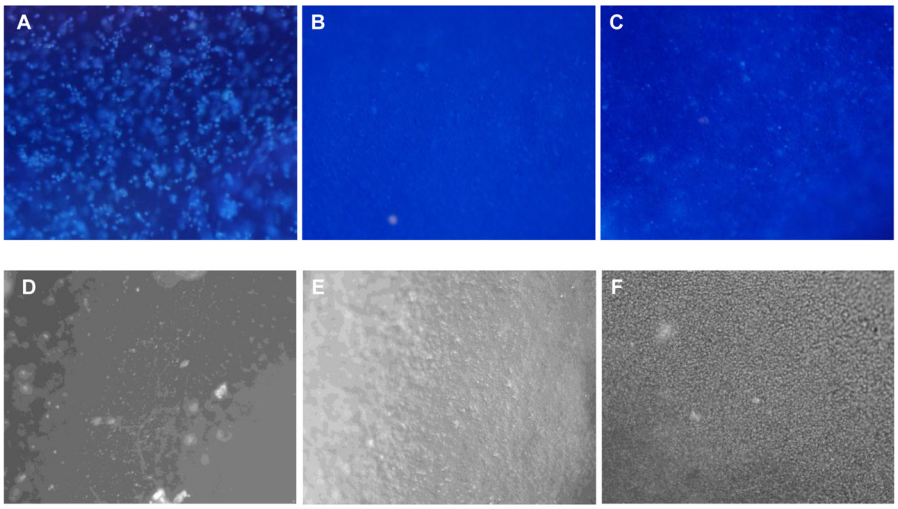


**Figure 10.**

Representative Alcian blue staining of primary bovine chondrocytes after 9 days of culture in HA-GMA gels (A), HA-*p*-HGP gels (B) and HA-c-HGP gels (C). Cell free hydrogels (D: HA-GMA; E: HA-*p*-HGP; F: HA-*c*-HGP) were included as the controls. Magnification: 10x.

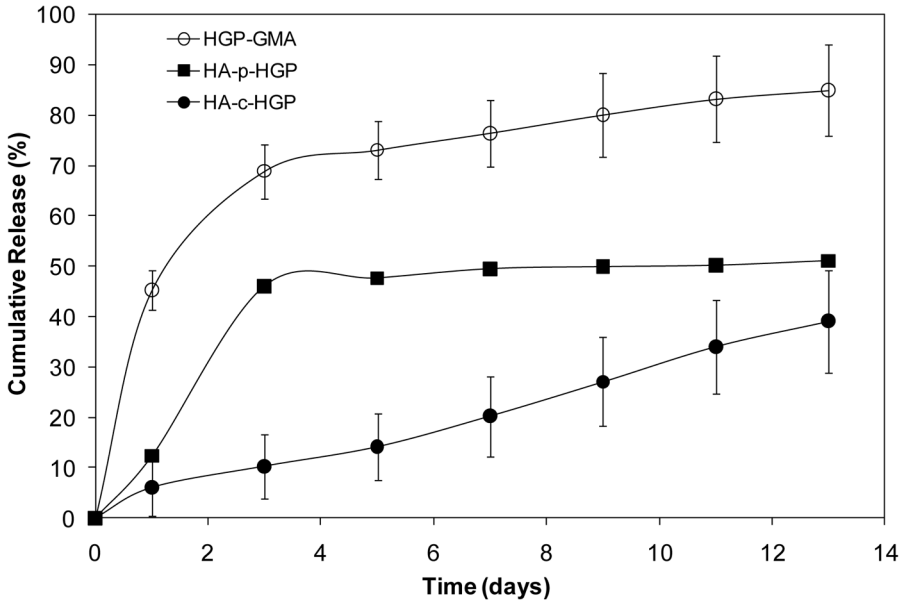


**Figure 11.**

BMP-2 release from HGP (○), HA-*p*-HGP gels (■) and HA-*c*-HGP gels (●). BMP-2 loaded HGPs were used for the formation of HA-*p*-HGP and HA-*c*-HGP gels. The hydrogel particles or the gel disks were incubated in the release buffer for up to 15 days and BMP-2 release was monitored using BMP-2 ELISA. BMP-2 release was calculated as the percentage of BMP-2 released at the indicated time relative to the amount bound to the particles at time 0. BMP-2 release from HGP–GMA, HA-*p*-HGP and HA-*c*-HGP was significantly different from one another at all times, $p \leq 0.05$.